Atmos. Meas. Tech. Discuss., 6, 2857–2905, 2013
www.atmos-meas-tech-discuss.net/6/2857/2013/
doi:10.5194/amtd-6-2857-2013

Atmospheric Measurement Techniques Discussions
Open Access

Microwave radiometer to retrieve temperature profiles from the surface to the stratopause

O. Stähli[1], A. Murk[1], N. Kämpfer[1,2], C. Mätzler[1,2], and P. Eriksson[3]

[1]Institute of Applied Physics, University of Bern, Bern, Switzerland
[2]Oeschger Centre for Climate Change Research, University of Bern, Bern, Switzerland
[3]Department of Earth and Space Sciences, Chalmers University of Technology, Göteborg, Sweden

Received: 6 March 2013 – Accepted: 15 March 2013 – Published: 21 March 2013

Correspondence to: O. Stähli (oliver.staehli@iap.unibe.ch)

Published by Copernicus Publications on behalf of the European Geosciences Union.

Abstract

TEMPERA is a new ground-based radiometer which measures in a frequency range from 51–57 GHz radiation emitted by the atmosphere. The instrument operates thermally stabilized inside a lab. With this instrument it is possible to measure temperature profiles from ground to about 50 km. This is the first ground-based instrument with the capability to retrieve temperature profiles simultaneously for the troposphere and stratosphere. The measurement is done with a filterbank in combination with a digital Fast-Fourier-Transform spectrometer. A hot load and a noise diode are used as stable calibration sources. The optics consist of an off-axis parabolic mirror to collect the sky radiation. Due to the Zeeman effect on the emission lines used, the maximum height for the temperature retrieval is about 50 km. The effect is apparent in the measured spectra. The performance of TEMPERA is validated by comparison with nearby radiosonde and satellite data from the Microwave Limb Sounder on the Aura satellite. In this paper we present the design and measurement method of the instrument followed by a description of the retrieval method, together with a validation of TEMPERA data over its first year, 2012.

1 Introduction

Temperature is a key parameter for dynamical, chemical and radiative processes in the atmosphere. There exist several techniques to measure atmospheric temperature profiles like radiosonde, FTIR, LIDAR or satellite and ground-based microwave radiometers. The advantage of ground-based radiometry is the high time resolution at a fixed location that allows to observe local atmospheric dynamics over a long time period.

In the troposphere the atmospheric temperature is important for weather fore- and now-casting. Ground-based microwave radiometers for tropospheric temperature profiles are well established and exist in different configurations. Examples are MICCY

AMTD
6, 2857–2905, 2013

(Crewell et al., 2001), RPG-HATPRO (Rose et al., 2005), Radiometrics MP-3000A (Ware et al., 2003) and ASMUWARA (Martin et al., 2006).

In the stratosphere temperature can influence chemical processes, and the vertical temperature distribution is important for atmospheric studies to investigate for example ozone or water vapor. The middle atmospheric temperature profile also can be affected by dynamical processes such as during Sudden Stratospheric Warming (SSW) events when the temperature in the stratosphere can change by several tens of degrees within a very short time. Therefore it is necessary to obtain temperature profiles with a good temporal and spatial resolution. At present, data of stratospheric temperature profiles are mostly obtained by remote sensing methods using radiometers on satellites (e.g. MLS instrument on the Aura satellite as described in Waters et al. (2006), AMSU-A instrument on the Aqua satellite as described in Aumann et al. (2003) and SABER instrument on the TIMED satellite as described in Remsberg et al., 2003). Satellite instruments do not measure always at the same place, and therefore ground-based microwave radiometers are a good complement. With ground-based instruments it is possible to investigate fast local atmospheric processes.

The possibility of ground-based measurements of stratospheric thermal emission from high-rotational, magnetic dipole transitions of molecular oxygen around 53 GHz was firstly shown in Waters (1973). It is interesting to note that no realization of a ground-based stratospheric temperature radiometer was reported in the literature for several decades. A recent realization of such an instrument was described by Shvetsov et al. (2010).

In this paper we describe the construction, calibration and utilization of a new ground-based TEMPERature RAdiometer, called TEMPERA, that is able to monitor temperature structures from ground to the upper stratosphere.

Other microwave radiometers in our group, like MIAWARA (Deuber et al., 2004) and MIAWARA-C (Straub et al., 2010) for water vapor profiles and GROMOS (Calisesi et al., 2001) for ozone profiles, can now use local atmospheric temperature profiles from TEMPERA. Most of these instruments and TEMPERA are located in Bern,

AMTD
6, 2857–2905, 2013

Switzerland (575 m a.s.l., 46.95° N/7.44° E). Two of them, MIAWARA and GROMOS, are operated within NDACC (Network for the Detection of Atmospheric Composition Change).

In the following section of this paper we present the measurement method and the instrumental set-up of TEMPERA. In the third section we describe the temperature retrieval. In the fourth section a validation of the TEMPERA data and comparison with radiosonde and satellite data is presented.

2 Measurement method and instrument description

2.1 Measurement method

TEMPERA measures thermal radiation from 51–57 GHz in the oxygen-emission region of the microwave spectrum. Oxygen is a well-mixed gas, whose fractional concentration is independent of altitude below approx. 80 km. Therefore the radiation contains information primarily on atmospheric temperature.

For tropospheric temperature profiles we measure with a filterbank at 12 frequencies from 51–57 GHz on the wing of the 60 GHz oxygen emission complex. In addition, with a digital Fast-Fourier-Transform (FFT) spectrometer, we get information on the temperature profile in the stratosphere by measuring two pressure-broadened emission lines centered at 52.5424 and 53.0669 GHz.

In microwave radiometry the measured intensity of radiation is often expressed as brightness temperature T_B according to the Rayleigh–Jeans-approximation of Planck's law. A ground-based microwave radiometer measures a superposition of emission and absorption of radiation at different altitudes. The intensity I can be described with the radiative transfer equation:

$$I(\nu,0) = I_0 e^{-\tau(\nu,s_0)} + \int_0^{s_0} B(\nu,T(s)) e^{-\tau(\nu,s)} \alpha(\nu,s) \mathrm{d}s, \quad (1)$$

AMTD
6, 2857–2905, 2013

where $I(\nu,0)$ is the measured intensity at frequency ν from an observation position 0 at the earth surface, I_0 is the microwave background intensity, s_0 is the position of the upper boundary of the atmosphere, $T(s)$ is the physical temperature and $\alpha(\nu,s)$ is the frequency dependent absorption coefficient both along the integration path s. $B(\nu,T)$ is the Planck function:

$$B(\nu,T) = \frac{2h\nu^3}{c^2}\frac{1}{e^{\frac{h\nu}{kT}}-1}, \tag{2}$$

where h is the Planck's constant, k is the Boltzmann's constant and c is the speed of light.

The opacity or optical depth τ is defined as:

$$\tau(\nu,s) = \int_0^s \alpha(\nu,s')\mathrm{d}s'. \tag{3}$$

Finally with the Rayleigh–Jeans limit (valid for the case $h\nu \ll kT$) we can calculate the measured brightness temperature T_B:

$$T_\mathrm{B}(\nu,0) = \frac{\lambda^2}{2k}I(\nu,0), \tag{4}$$

where λ is the wavelength.

The measured spectrum $T_\mathrm{B}(\nu,0)$ is used to retrieve the temperature profile as described in Sect. 3.1.

2.2 Instrumental description

TEMPERA is a heterodyne receiver at a frequency range of 51–57 GHz. Figures 1 and 2 give an overview of the instrument and its specifications. Our instrument consists of three parts: the frontend to collect and detect the microwave radiation with two

AMTD
6, 2857–2905, 2013

backends, a filterbank and a digital FFT spectrometer for the spectral analysis. The radiation is directed into the corrugated horn antenna using an off-axis parabolic mirror. The antenna beam has a Half Power Beam Width (HPBW) of 4°. The signal is then amplified and downconverted to an intermediate frequency for further spectral analysis. A noise diode in combination with an ambient hot load is used for calibration. The receiver noise temperature T_N is in a range from 475–665 K. An overview of the technical specifications is given in Table 1.

For the tropospheric measurements we use a filterbank with 4 channels. In the end we measure at 12 frequencies which are listed in Table 2 by adjusting the local oscillator (LO) frequency with a synthesizer. For every measured zenith angle the LO frequency is changed three times. In this way we cover uniformly the range from 51–57 GHz at positions between the emission lines (see Fig. 3). The lower 9 channels have a bandwidth of 250 MHz and the channels 10–12 have a bandwidth of 1 GHz to enhance the sensitivity in the flat spectral region.

The second backend is used for stratospheric measurements and contains a digital FFT spectrometer (Acqiris AC 240) for the two emission lines centered at 52.5424 and 53.0669 GHz. The input signal is coupled from the main signal before the filterbank. It passes an IQ-Mixer before being fed to the spectrometer. When the LO frequency is changed by the synthesizer in the frontend the second synthesizer, which is placed in front of the IQ-Mixer, also changes the frequency. With this method we can always measure the same range with the FFT spectrometer. Further this allows us to measure the tropospheric and stratospheric part at the same time. With the FFT spectrometer in combination with the IQ-Mixer we can measure the two emission lines with a resolution of 30.5 kHz and a bandwidth of 960 MHz. The receiver noise temperature T_N for the receiver-spectrometer combination is around 480 K. The details are listed in Table 2.

An example of a measured spectrum is shown in Fig. 4. The zoomed lines show the influence of the Zeeman effect by the broadened line shape in the center with a kind of a plateau (round line shape around the line center: ±1 MHz).

AMTD
6, 2857–2905, 2013

TEMPERA operates from a temperature-stabilized laboratory at the ExWi Building of the University of Bern (Bern, Switzerland: 575 m a.s.l.; 46.95° N/7.44° E, view direction in azimuth: south-east (131.5°)). A styrofoam window allows views of the atmosphere over the zenith angle (za) range from 30° to 70°. The operation of the instrument inside a laboratory has the advantage that the radiometer is protected against adverse weather conditions. The frontend itself has additional temperature stabilization with Peltier elements in combination with a ventilation system leading to a stabilization of the frontend plate within ±0.2 K.

2.3 Measurement cycle

Measurements are performed in periodic cycles with periods of 60 s. Each cycle starts with hot load calibration in combination with a noise diode (see also Sect. 2.4) for 9 s followed by the atmosphere measurements. They consist of two parts: first a 15 s period at a zenith angle za = 30° to observe with the FFT spectrometer and simultaneously with the filterbank, and second, a tipping curve in 3 s periods and angular steps in 5° up to za = 70°.

After calibration, the output of each measurement cycle is a set of 108 brightness temperatures of the filterbank at 12 frequencies and at 9 zenith angles and a calibrated spectrum at the two emission lines from the FFT spectrometer consisting of 32 768 channels covering the bandwidth of 960 MHz.

For the retrieval we use a mean of 15 measurement cycles for the troposphere and 120 measurement cycles for the stratosphere leading to a time resolution of 15 min for tropospheric profiles and 120 min for stratospheric profiles.

2.4 Calibration

Under the assumption of linearity between the antenna temperature T_A and the detector-output voltage V_{TA}, and furthermore under the assumption of a perfect antenna that the brightness temperature T_B is equal to T_A the following relation is valid:

AMTD
6, 2857–2905, 2013

$$T_B = T_A = \frac{V_{TA}}{g} - T_N \quad (5)$$

where g is the effective gain factor and T_N is the receiver noise temperature.

The calibration parameters g and T_N are obtained from the known radiation of an ambient hot load in combination with a noise diode.

To calibrate the noise diode we use a hot and a cold load. The cold load is a microwave absorber dipped in liquid nitrogen. Both loads are pyramidal microwave absorbers. With this calibration the so-called excess-noise diode temperature T_{ND} is determined:

$$T_{ND} = (T_H - T_C) \cdot \frac{V_{HND} - V_H}{V_H - V_C} \quad (6)$$

where T_H is the physical temperature of the hot load, T_C is the physical temperature of the cold load (around 77 K at a altitude of 575 m, depending on pressure), V is the detector-output voltage, index H means hot load, HND hot load with the noise diode switched on, and C cold load, respectively.

The excess-noise diode temperature T_{ND} is in a range from 40–75 K depending on the frequency.

With T_{ND} we can finally calculate g and T_N:

$$g = \frac{V_{HND} - V_H}{T_{ND}} \quad (7)$$

$$T_N = \frac{V_H \cdot (T_H + T_{ND}) - V_{HND} \cdot T_H}{V_{HND} - V_H} \quad (8)$$

The excess-noise diode temperature T_{ND} is normally stable over several weeks ($\Delta T_{ND} < 0.3$ K for all frequencies). Therefore we repeat its calibration with liquid nitrogen every month.

AMTD
6, 2857–2905, 2013

3 Temperature retrieval

3.1 Retrieval

Our temperature retrieval is based on the Optimal Estimation Method (OEM) (Rodgers, 2000). The forward model F as expressed by Eqs. (1) and (4) is used to simulate our measured brightness temperature. Here we express it in the following equation:

$$\boldsymbol{y} = F(\boldsymbol{x}, \boldsymbol{b}) + \epsilon \tag{9}$$

where the vector $\boldsymbol{y}$ is the measured spectrum (brightness temperature), $\boldsymbol{x}$ is the true temperature profile, $\boldsymbol{b}$ contains some additional forward model parameters, and ϵ is the measurement noise. In our case F is non-linear. To retrieve the temperature profile from the measured brightness temperature Eq. (9) has to be inverted. This is an ill-posed problem because the solution is not unique. To handle this problem we have to find an optimal solution that is defined by the zero of the gradient of the cost function J:

$$J = [\boldsymbol{y} - F(\boldsymbol{x})]^T \mathbf{S}_\epsilon^{-1} [\boldsymbol{y} - F(\boldsymbol{x})] + [\boldsymbol{x} - \boldsymbol{x}_\mathrm{a}]^T \mathbf{S}_\mathrm{a}^{-1} [\boldsymbol{x} - \boldsymbol{x}_\mathrm{a}] \tag{10}$$

where $\boldsymbol{x}_\mathrm{a}$ is the a-priori temperature profile, $\mathbf{S}_\mathrm{a}$ is the a-priori covariance matrix and $\mathbf{S}_\epsilon$ is the measurement error-covariance matrix.

This principle is based on Bayes' probability theorem, giving the solution with the highest probability and constraining the solution to realistic profiles with a-priori knowledge. To find the zero of the derivative we use the Gauss–Newton iterative method leading to:

$$\boldsymbol{x}_{i+1} = \boldsymbol{x}_i + \left(\mathbf{S}_\mathrm{a}^{-1} + \mathbf{K}_i^T \mathbf{S}_\epsilon^{-1} \mathbf{K}_i\right)^{-1} \left[\mathbf{K}_i^T \mathbf{S}_\epsilon^{-1} (\boldsymbol{y} - F(\boldsymbol{x}_i)) - \mathbf{S}_\mathrm{a}^{-1} (\boldsymbol{x}_i - \boldsymbol{x}_\mathrm{a})\right] \tag{11}$$

where $\boldsymbol{x}_i$ is the retrieved temperature profile at iteration i and $\mathbf{K}$ is the weighting function ($\mathbf{K} = \partial F / \partial \boldsymbol{x}$).

AMTD
6, 2857–2905, 2013

The radiative transfer calculations are done with the Atmospheric Radiative Transfer Simulator 2 (ARTS2, Eriksson et al., 2011). The inversion is treated in Qpack2 (Eriksson et al., 2005).

The retrieval is calculated on a pressure grid. In this paper all data are plotted in geometric height in km for practical reasons. For the conversion from a pressure grid to a kilometer grid we used radiosonde and ECMWF (European Centre for Medium-Range Weather Forecasts) data.

In the OEM method an often used tool is the averaging kernel matrix **A** (Rodgers, 2000) that describes the response of the retrieved temperature profile $\hat{\boldsymbol{x}}$ to a change in the "true" profile $\boldsymbol{x}$.

$$\mathbf{A} = \mathbf{D}_y \mathbf{K}_x = \frac{\partial \hat{\boldsymbol{x}}}{\partial \boldsymbol{x}} \tag{12}$$

where $\mathbf{K}_x = \partial F / \partial \boldsymbol{x}$ is the weighting function matrix and $\mathbf{D}_y = \partial \hat{\boldsymbol{x}} / \partial \boldsymbol{y}$ the contribution function.

The rows of **A** are called the averaging kernels (AVK). Every row describes the sensitivity of the retrieval for a certain height level to a perturbation at other levels. The sum of the AVK is called the Measurement Response (MR) which describes the contribution of measurement to the retrieved profile at a certain height. The full-width at half-maximum (FWHM) of the AVK is often used as a height resolution of the retrieval.

To compare profiles from a ground-based radiometer with a reference profile from collocated radiosonde and satellite there exist different methods. One possibility is to interpolate the reference profiles at levels of the radiometer and compare it directly. A second method is to convolve the interpolated reference profile $\boldsymbol{x}_\mathrm{r}$ with the Averaging Kernel **A** of the radiometer to take into account the different height resolutions:

$$\hat{\boldsymbol{x}}_\mathrm{r} = \boldsymbol{x}_\mathrm{a} + \mathbf{A}(\boldsymbol{x}_\mathrm{r} - \boldsymbol{x}_\mathrm{a}) \tag{13}$$

where $\boldsymbol{x}_\mathrm{a}$ is the a-priori profile of the radiometer.

AMTD
6, 2857–2905, 2013

3.2 Forward model parameters

In the radiative transfer calculations we use the models of Rosenkranz and Liebe for the absorption coefficient calculations: Rosenkranz (1998) for H_2O, Rosenkranz (1993) for O_2 and Liebe et al. (1993) for N_2. The used line parameters for the oxygen (O_2) spectral lines are listed in Table 3.

In the forward model a water-vapour profile with an exponential decrease is included. This profile is calculated with the measured surface water vapor density from the ExWi-Weather station (placed next to TEMPERA) and assuming a scale height of 2500 m. Further descriptions can be found in Bleisch et al. (2011). For other species like oxygen (O_2) and nitrogen (N_2) we used standard atmospheric profiles for summer and winter which are incorporated in ARTS2 (middle latitude FASCOD, Anderson et al., 1986).

The presence of clouds has a relatively strong influence in the frequency range from 51 to 53 GHz as can be seen in Fig. 5. In this figure the absorption coefficient for water vapor, liquid water, nitrogen and oxygen for 5 different frequencies between 51 and 57 GHz is plotted. The absorption coefficient of the nitrogen, water vapor and the liquid water is more or less the same for the 5 frequencies. This is not true for oxygen which is strongly dependent on frequency. Furthermore the figure shows that cloud liquid has a similar absorption coefficient as oxygen in the frequency range from 51 to 53 GHz. On the other hand during clear sky (ILW = 0 mm) the main part of the absorption and emission in the atmosphere is from oxygen dominating the contribution from water vapor and nitrogen. Further discussion about temperature retrieval during weather conditions with and without clouds will be presented in Sect. 4.2.

3.3 Weighting functions

Accurate and rapid calculations of weighting functions (WFs) are important for obtaining stable and fast inversions. Both aspects point towards using analytical expressions as far as possible, and this is also the case in ARTS (Buehler et al., 2005). However, a total general expression for temperature WFs can hardly be derived and ARTS

AMTD
6, 2857–2905, 2013

has previously resorted to perturbations calculations for these WFs. Motivated by this project, analytically-based options have been re-examined.

The derived expressions are reported in the ARTS user guide (www.sat.ltu.se/arts/docs). The expressions cover all significant local effects, but ignore non-local impacts that can occur through refraction and hydrostatic equilibrium. These mechanisms give a coupling between the local temperature and the propagation path through other atmospheric layers, that for e.g. limb sounding can be highly important. On the other hand, ignoring non-local effects is an acceptable approximation for ground-based observations as long as the elevation angle is above $\approx 20^{\circ}$, for reasons discussed in the user guide.

A further consideration is that the WFs assume that other model state variables are kept constant. This has the consequence that the exact expression will differ depending on whether the gas abundances is given as number density, volume mixing ratio or some other unit. ARTS applies volume mixing ratio, which is the natural choice for oxygen.

In summary, ARTS can now calculate temperature WFs with a much lower calculation cost by applying analytical expressions. The obtained analytical WFs are practically identically to reference perturbation calculations for the measurements of concern here.

3.4 Error analysis

The total random error of a retrieval consists mainly of the observation error, due to the measurement noise and uncertainty and of the smoothing error, caused by the vertical smoothing of the retrieval method. The estimation of the observation covariance matrix ($\mathbf{S}_o$) and the smoothing covariance matrix ($\mathbf{S}_s$) are shown in the following equations (Rodgers, 2000):

$$\mathbf{S}_o = \mathbf{D}_y \mathbf{S}_e \mathbf{D}_y^T \quad (14)$$

$$\mathbf{S}_s = (\mathbf{A} - \mathbf{I})\mathbf{S}_a(\mathbf{A} - \mathbf{I})^T \quad (15)$$

AMTD
6, 2857–2905, 2013

where **I** is the identity matrix. The total random error of the observation and of the vertical smoothing is calculated as the square root of the diagonal elements of the covariance matrix $\mathbf{S}_o$ and $\mathbf{S}_s$, respectively.

3.5 Tropospheric retrieval

As mentioned before, to retrieve tropospheric temperature profiles 12 channels are used (Table 2). Additionally we get information from 9 zenith angles (30° to 70°, every 5°).

The retrieval software Qpack2 (Eriksson et al., 2005) uses a pressure grid for the retrieval calculations. Our first pressure-grid point is at the surface where our instrument is situated. This pressure value is taken from our weather station at the measurement time. The other grid points are selected in such a way that we have more grid points in the lower troposphere than in the upper troposphere, because the measurements contains most information from the lowest layers of the troposphere. Our grid has a resolution of about 100 m from ground to 1 km, about 300 m from 1 to 5 km and about 500 m from 5 to 10 km.

As an a-priori temperature profile monthly mean radiosonde data from Payerne (46.82° N/6.95° E; 491 m a.s.l. and 40 km W of Bern) are used. The data are from 1994 to 2011 and the soundings are twice a day at 11:00 and at 23:00 (UT). For the a-priori covariance matrix $\mathbf{S}_a$ we use a correlation function decreasing exponentially with a correlation length of 3 km. A standard deviation of 2 K at ground decreasing linearly to 1.5 K at 15 km is assumed. The measurement error is considered in the covariance matrix $\mathbf{S}_\epsilon$ as a diagonal matrix. Normally we retrieve every 15 min a temperature profile (96 profiles per day) and therefore we use the standard deviation of around 15 measurements (1 measurement cycle: 1 min) at every zenith angle and frequency. The measurement error is normally in a range of 0.4 to 2 K depending on frequency, zenith angle and weather conditions.

AMTD
6, 2857–2905, 2013

3.6 Stratospheric retrieval

The stratospheric temperature profile is retrieved from the measurement of the two emission lines, centered at 52.5424 and 53.0669 GHz. We use the two lines at the same time with a bandwidth of 200 MHz around 52.5424 GHz and 160 MHz around 53.0669 GHz. With the digital FFT spectrometer we measure at a zenith angle of 30°. In Fig. 3 simulated spectra at the three different zenith angles 30°, 50° and 70° can be seen. The results show that the intensity of the emission lines is highest at za = 30°. Therefore we decided to measure the emission lines at this angle.

During a measurement cycle the integration time with the FFT spectrometer is 15 s. For a temperature profile we integrate the measurement for half an hour because then the noise level is low enough to get good retrievals. This requires two hours of measurement time, because only one quarter of the measurement time is spent for the digital FFT spectrometer. The remaining period of the measurement TEMPERA measures at za = 35–70° with the filterbank only (see also Sect. 2.3). For the forward model we use a vertical grid with a resolution of about 350 m. Further in the forward model ±1 MHz around the two line centers we have no frequency points in the grid, because the Zeeman effect is not yet fully incorporated in Qpack2/ARTS2. In the center of the lines (±16 MHz, 1000 channels) we use all channels, and on the wings of the line we use a binning of 3 channels for data reduction.

As a temperature a-priori profile from ground to about 15 km we use a monthly mean of radiosonde data from Payerne from 1994 to 2011. Above, a climatology of the Microwave Limb Sounder (MLS) data (Aura satellite) is used. For the a-priori covariance matrix $\mathbf{S}_a$ we use a correlation function decreasing exponentially with a correlation length of 3 km. A standard deviation of 2 K is assumed. The measurement error (residual) is considered in the covariance matrix $\mathbf{S}_\epsilon$ as a diagonal matrix. The residual is the difference between the integrated spectra and the fit of the spectra. Under regular conditions the measurement error is in a range from 0.5 to 1 K. Around 52.5424 GHz

AMTD
6, 2857–2905, 2013

(first line) the noise is higher than around at 53.0669 GHz (second line), as shown in Fig. 4.

Normally we retrieve a temperature profile every 2 h resulting in 12 profiles per day. The retrieval works fine for Integrated Liquid Water ILW ≤ 0.1 mm. For larger values the retrieval is suppressed.

4 Temperature profiles: results

4.1 Introduction

Here we present an analysis of temperature retrievals from TEMPERA over almost one year, during the period from 1 January to 13 December 2012. The data consist of 2929 stratospheric profiles and 33 021 tropospheric profiles. The whole data set, covering the height range from ground to 50 km, can be seen in Fig. 6. The white lines indicate the measurement response MR = 0.6. The altitude range with MR ≥ 0.6 is from ground to 5–6 km (troposphere) and from 18 to 48 km (stratosphere). The troposheric data are during all-weather conditions, and the stratospheric data are during conditions with ILW ≤ 0.1 mm to avoid effects due to clouds. The information about clouds (ILW) are from the radiometer TROWARA (Mätzler and Morland, 2009) that is installed next to TEMPERA, measuring the radiation from the sky in the same direction at 21, 22 and 31 GHz.

More details about the tropospheric and stratospheric temperature profiles will follow in the next sections. Furthermore comparison between the data of TEMPERA and radiosonde and satellites data will be discussed.

AMTD
6, 2857–2905, 2013

4.2 Tropospheric temperature profiles

4.2.1 Clear sky measurements

Figure 7 shows a typical result of a temperature profile (upper plot) at times without liquid water compared with the profile as obtained by a nearby radiosounding and the used a-priori profile. Further the corresponding brightness temperatures (lower plot) from 14 November 2011 at 11:00 (UT) is shown. In this case we use all 12 channels and 9 zenith angles with a total of 108 measured brightness temperatures.

At this time there was an inversion between 1000 m and about 3000 m. Nevertheless the retrieved temperature profile from TEMPERA measurements agrees well with the radiosonde profile from Payerne and the weather stations from Bern and Zimmerwald (46.88° N/7.47° E; 905 m a.s.l. and 10 km S of Bern).

The forward model brightness temperatures, calculated for the retrieved profile, agree well with the measured brightness temperatures for all channels. The absolute difference between measured and forward model brightness temperatures (residuals) is between 0.05 and 1.2 K. The averaging kernels, the height resolution (FWHM of the averaging kernels) and the measurement response are shown in Fig. 8. The height resolution in the first kilometer is about 300 m. From 1 to 10 km the height resolution increases to around 5 km.

The retrieval error, calculated with Eqs. (14) and (15), is shown in Fig. 8. The total error is less than 0.5 K from ground to 1 km and then is increasing linearly to 1.5 K at 10 km. Further it is seen that the measurement error is much smaller than the smoothing error.

This example shows that during clear sky we get good results compared with the radiosondes and weather stations from ground up to 7 km with a measurement response higher than 0.6. From 7 km to 10 km the measurement response is smaller than 0.6 and more information from the a-priori profile is used than from the measurements.

AMTD
6, 2857–2905, 2013

4.2.2 Measurements with cloudy sky

To retrieve temperature profiles during cloudy sky the lowest 4 channels between 51.25–52.85 GHz are not taken into account in the calculations due to the unknown cloud influence shown in Fig. 5. We choose a threshold of ILW = 0.025 mm to use only 8 channels. Below this threshold value the retrieval takes into account all 12 channels. At the moment we do not take into account the liquid water (clouds) in the forward model. With this simple but effective method we get reasonable results.

A typical result of a temperature profile from 14 November 2011 at 23:00 (UT) with ILW = 0.1 mm is shown in Fig. 9. This measurement contains 8 frequencies (channels 5–12: 53.35–57 GHz) and 9 zenith angles providing 72 measured brightness temperatures (see also Fig. 9). The forward model brightness temperatures agree with the measured brightness temperatures. With an absolute difference between measured and forward model brightness temperatures (residuals) between 0.05 and 1.8 K. Also the temperature profile from TEMPERA agrees with the radiosonde data from Payerne and the weather station from Bern and Zimmerwald. The best agreements are in the altitude range from ground to about 2.5 km.

The averaging kernels, the height resolution (FWHM of the averaging kernels) and the measurement response are shown in Fig. 10. The height resolution is similar as for clear sky. During cloudy sky the measurement response is higher than 0.6 up to about 6 km, i.e. slightly less than during clear sky, because the unused channels carry information about the upper troposphere.

The retrieval error, calculated with Eqs. (14) and (15), is shown in Fig. 10. Also the retrieval error is similar to clear sky measurements.

4.2.3 Comparison with radiosonde data over time

We compared the TEMPERA tropospheric temperature profiles with the radiosonde data from Payerne over the period from 1 January to 13 December 2012 during all weather conditions. The comparison consists of 644 profiles. The data are restricted

AMTD
6, 2857–2905, 2013

to cases with near time-coincident sounding and retrieval profiles (normally two cases per day). Figure 11 shows a time-series at 5 altitude levels. We observe an excellent agreement below altitudes of about 1.5 km with a Correlation-Coefficent CC ≥ 0.97. From 1.5 km to about 5 km the results are still well correlated with CC ≥ 0.86. From 5 to 10 km the TEMPERA data agree fairly well with the data from radiosonde (0.77 ≤ CC ≤ 0.86). The mean and the standard deviation of the difference $T_{\text{TEMPERA}} - T_{\text{RS PAY}}$ are shown in Fig. 12 over the altitude range from ground to 10 km. Also this plot shows that the best agreement is from ground to about 1.5 km. The mean difference is between −0.5 K and +1 K over the whole altitude range. The standard deviation is around 1 K from ground to 1.5 km and is then increasing to nearly 3 K at 3 km and staying constant at this value until 10 km. A similar behavior of the mean value and standard deviation is seen in the comparison between TEMPERA data and convolved data of radiosondes from Payerne (see also Fig. 12 lower panel). In these data the agreements are better. Further the correlation coefficient of all levels for the unconvolved and convolved data are shown in Fig. 13.

This comparison shows that TEMPERA is measuring very well in the lower troposphere (ground–2 km) with CC ≥ 0.93 and with CC ≥ 0.96 for convolved data. In the upper troposphere the agreement is reasonably well (2–6 km: CC ≥ 0.86 and CC ≥ 0.89 for convolved data), but we also see in the results that TEMPERA is not very sensitive in a altitude range from 6–10 km (CC ≥ 0.77). This is also seen in the measurement response.

In Fig. 11 an interesting period in the dataset is during the first half of February 2012 over an altitude range from ground to about 2.5 km. During this time, in Switzerland, there was a strong cooling from about 280 K to 260 K at ground. A further interesting case was a warming during August 2012 with a temperature of almost 290 K at 2.5 km. Both effects were measured with TEMPERA and also with radiosonde data from Payerne.

AMTD
6, 2857–2905, 2013

4.3 Stratospheric temperatures profiles

A typical retrieved stratospheric temperature profile is seen in Fig. 14 for 15 June 2012 from 12:04 to 14:04 (UT). Over an altitude range from 20–45 km the profile agrees well with other measurements, i.e. satellite data from Aura/MLS and the radiosonde data from Payerne. Also the forward model brightness temperatures agree reasonably well with the measured brightness temperatures excepting around the line center. This is because of the Zeeman effect, that has not yet been incorporated in the forward model.

The averaging kernels, the height resolution (FWHM of the averaging kernels) and the measurement response are shown in Fig. 15. The height resolution is about 15 km. The measurement response higher than 0.6 is in a altitude range from 18 to 48 km. The retrieval error, calculated with Eqs. (14) and (15), is shown in Fig. 15. The total error is between 1.6 and 1.8 K in the altitude range of 18 to 48 km. Again, it is seen that the measurement error is much smaller than the smoothing error.

4.3.1 Comparison with radiosonde and satellite data over time

We compared the TEMPERA stratospheric temperature profiles with the radiosonde data from Payerne and with MLS data over the period from 1 January to 13 December 2012 during weather conditions with ILW $\leq$ 0.1 mm. The comparison between TEMPERA data and radiosondes from 10 to 29 km consists of 524 profiles. The data are restricted to cases with near time-coincident sounding and retrieval profiles (normally two cases per day). Figure 16 shows the time-series at 5 levels. The plot shows that, apart from some exceptions, the time evolution in temperature of both measurements is similar. The best agreement is found at altitudes between 25 and 29 km with a CC between 0.89 and 0.916. The mean and the standard deviation of the difference $T_{\mathrm{TEMPERA}} - T_{\mathrm{RS\ PAY}}$ with unconvolved and convolved data are shown in Fig. 17. The mean difference is between −1 K and 1 K, and the standard deviation is less than 3 K on an altitude range from 18 to 29 km. Again, the comparison is better with convolved

AMTD
6, 2857–2905, 2013

data (see also Fig. 17, lower panel). The correlation coefficient over all levels with and without convolved data are plotted in Fig. 20 in the upper panel.

Another comparison is obtained from MLS data with 243 profiles. The criterion for a collocation of a MLS profile with the measurement site is ±1° (±110 km) in latitude and ±5° (±460 km) in longitude. Further the plotted data are restricted to cases with near time-coincident MLS profiles and TEMPERA profiles. Figure 18 shows the timeseries at 5 levels from 25 to 45 km with a CC between 0.87 and 0.92. Also here we see that the time evolution in temperature is similar for both instruments. The mean of the difference $T_{\mathrm{TEMPERA}} - T_{\mathrm{MLS}}$ (see Fig. 19) is varying between 0 K and 1 K from 20 to 30 km followed by a dip to −2 K at 35 km and increasing to around 2 K at 45 km. The standard deviation of this comparison is around 2.5 K from 20 to 35 km and around 4.5 K above 35 km. The agreement between the TEMPERA data and the MLS convolved data are better with a CC ≥ 0.95 over altitude levels from 18 to 48 km (MR ≥ 0.6). The correlation coefficient over all levels with and without convolved data are plotted in Fig. 20 in the lower panel.

An interesting period was observed with TEMPERA and MLS in the beginning of January 2012 (Fig. 18). Both instruments measured a warming from about 260 to 280 K at an altitude of 45 km within some days. End of October and in the beginning of November there was a warming of more than 10 K at levels between 20 to 30 km. All three instruments (radiosonde, MLS and TEMPERA) measured these effects.

Both comparisons show that TEMPERA performs well in the stratosphere. The results are best in the range from 25 to 40 km with CC ≥ 0.9 and with CC ≥ 0.95 for convolved data.

4.3.2 Sudden Stratospheric Warming (SSW) over Bern during winter 2012/2013

At the end of 2012 and in the beginning of 2013 a Sudden Stratospheric Warming occured that also was observed over Bern. During a SSW the temperature in the stratosphere is increasing by several tens of degrees within a very short time. This type of warming was first observed by Scherhag (1952). In 2008 and 2010 SSW events over Bern were observed. Flury et al. (2009) and Scheiben et al. (2012) reported the

AMTD
6, 2857–2905, 2013

influence of the temperature increase on ozone and water vapor in the stratosphere measured with ground-based microwave radiometers. Both studies used temperature profiles from ECMWF or MLS to investigate the SSW.

With TEMPERA we measured the recent SSW event. The timeseries from 21 December 2012 to 4 February 2013 (46 days) is shown in Fig. 21. In this plot we see a strong warming by about 30 K at an altitude of 40 km in the time period from 21 December 2012 to 25 December 2012. The warming stayed with temperatures between 250 to 290 K until 12 January 2013 over the altitude range of 40 km to 50 km. The warmest region with 290 K was near 45 km. After this time period the temperature decreased to temperatures between 240 to 265 K.

This example shows that with TEMPERA it is possible to measure such interesting stratospheric events and to study local phenomena at mesoscale. Furthermore it is possible to investigate this SSW with profiles from our ground-based microwave instruments for temperature, ozone and water vapor.

5 Conclusions

TEMPERA is a new ground-based radiometer for tropospheric and stratospheric temperature profiles. For the troposphere a filterbank with 12 channels (51–57 GHz) is used and for the stratosphere two emission lines at 52.5424 and 53.0669 GHz are measured with a digital FFT spectrometer. This radiometer is the first instrument to measure temperature profiles from ground to about 50 km with a high sensitivity from ground to 6 km and from 18 to 48 km. From 6 to 18 km we also get information from our measurements for the temperature profiles but with reduced sensitivity meaning that we use more information from the a-priori profile.

First validations of TEMPERA data with radiosonde and satellite data showed good agreements. The comparison of 644 profiles in the troposphere with radiosonde showed that the mean difference of the data is between −0.5 K and 1 K with a Correlation Coefficient CC ≥ 0.93 (convolved data: CC ≥ 0.96) from ground to 2 km, a CC ≥

AMTD
6, 2857–2905, 2013

0.86 (convolved data: CC ≥ 0.89) from 2 to 6 km and from 6 to 10 km the CC is between 0.77 and 0.86.

Also the comparison in the stratosphere with radiosonde (524 profiles) and satellite data (243 profiles) are good. In the stratosphere the mean difference is between −2 K and 2 K. The results are best in the range from 25 to 40 km with CC ≥ 0.9 and with CC ≥ 0.95 for convolved data. During cloudy sky there is a simple way to improve the tropospheric retrieval by only using the higher frequencies above 53 GHz. For the stratospheric temperature retrieval we limited the retrievals to IWV ≤ 0.1 mm.

The upper height limit of the retrieval is at 50 km due to the Zeeman effect. This effect is also seen in the measurements with the digital FFT spectrometer as a line broadening nearby the line center.

The data in this paper were produced with two independent retrievals for the troposphere and the stratophere and merged then together in a colorplot over a altitude range from ground to 50 km. In the future our goal is to combine the two datasets to a single retrieval to get one profile from ground to 50 km. Furthermore for future work we want to investigate in more detail the retrieval under cloudy conditions (liquid clouds only). Furthermore it is aimed to measure the Zeeman effect with a narrowband software-defined radio (SDR) spectrometer. The effect will be incorporated in the forward model to improve the stratospheric temperature retrieval.

Acknowledgements. This work has been supported by the Swiss National Science Foundation grant number 200020-134684. Balloon sounding profiles were kindly provided by MeteoSwiss, Payerne. We thank NASA for making Aura MLS data available.

AMTD
6, 2857–2905, 2013

References

Anderson, G. P., Clough, S. A., Kneizys, F. X., Chetwynd, J. H., and Shettle, E. P.: AFGL atmospheric constituent profiles (0–120 km), Tech. rep., Tech. Rep. TR-86-0110, AFGL, 1986. 2867

Aumann, H. H., Chahine, M. T., Gautier, C., Goldberg, M. D., Kalnay, E., McMillin, L. M., Revercomb, H., Rosenkranz, P. W., Smith, W. L., Staelin, D. H., Strow, L. L., and Susskind, J.: AIRS/AMSU/HSB on the Aqua mission: design, science objectives, data products, and processing systems, IEEE T. Geosci. Remote., 41, 253–264, doi:10.1109/TGRS.2002.808356, 2003. 2859

Bleisch, R., Kämpfer, N., and Haefele, A.: Retrieval of tropospheric water vapour by using spectra of a 22 GHz radiometer, Atmos. Meas. Tech., 4, 1891–1903, doi:10.5194/amt-4-1891-2011, 2011. 2867

Buehler, S. A., Eriksson, P., Kuhn, T., von Engeln, A., and Verdes, C.: ARTS, the Atmospheric Radiative Transfer Simulator, J. Quant. Spectrosc. Ra., 91, 65–93, doi:10.1016/j.jqsrt.2004.05.051, 2005. 2867

Calisesi, Y., Wernli, H., and Kämpfer, N.: Midstratospheric ozone variability over Bern related to planetary wave activity during the winters 1994–1995 to 1998–1999, J. Geophys. Res., 106, 7903–7916, 2001. 2859

Crewell, S., Czekala, H., Löhnert, U., Simmer, C., Rose, T., and Zimmermann, R.: Microwave radiometer for cloud cartography, a 22-channel ground-based microwave radiometer for atmospheric research, Radio Sci., 36, 621–638, 2001. 2859

Deuber, B., Kämpfer, N., and Feist, D. G.: A new 22-GHz radiometer for middle atmospheric water vapor profile measurements, IEEE T. Geosci. Remote, 42, 974–984, 2004. 2859

Eriksson, P., Jiménez, C., and Buehler, S. A.: Qpack, a general tool for instrument simulation and retrieval work, J. Quant. Spectrosc. Ra., 91, 47–64, doi:10.1016/j.jqsrt.2004.05.050, 2005. 2866, 2869

Eriksson, P., Buehler, S. A., Davis, C. P., Emde, C., and Lemke, O.: ARTS, the atmospheric radiative transfer simulator, Version 2, J. Quant. Spectrosc. Ra., 112, 1551–1558, doi:10.1016/j.jqsrt.2011.03.001, 2011. 2866

Flury, T., Hocke, K., Haefele, A., Kämpfer, N., and Lehmann, R.: Ozone depletion, water vapor increase, and PSC generation at midlatitudes by the 2008 major stratospheric warming, J. Geophys. Res., 114, D18302, doi:10.1029/2009JD011940, 2009. 2876

AMTD
6, 2857–2905, 2013

Liebe, H., Hufford, G., and Cotton, M.: Propagation modeling of moist air and suspended water/ice particles at frequencies below 1000 GHz, in: AGARD 52nd Specialists Meeting of the Electromagnetic Wave Propagation Panel, Palma de Mallorca, Spain, 3.1–3.10, 1993. 2867

Martin, L., Schneebeli, M., and Mätzler, C.: ASMUWARA, a ground-based radiometer system for tropospheric monitoring, Meteorol. Z., 15, 11–17, doi:10.1127/0941-2948/2006/0092, 2006. 2859

Mätzler, C. and Morland, J.: Refined physical retrieval of integrated water vapor and cloud liquid for microwave radiometer data, IEEE T. Geosci. Remote, 47, 1585–1594, 2009. 2871

Remsberg, E. E., Lingenfelser, G., Harvey, V. L., Grose, W., Russell III, J. M., Mlynczak, M. G., Gordley, L., and Marshall, B. T.: On the verification of the quality of SABER temperature, geopotential height, and wind fields by comparison with MET Office assimilated analyses, J. Geophys. Res., 108, 1–10, doi:10.1029/2003JD003720, 2003. 2859

Rodgers, C. D.: Inverse Methods for Atmospheric Soundings, World Scientific Publishing Co Pte. Ltd, Singapore, 2000. 2865, 2866, 2868

Rose, T., Crewell, S., Löhnert, U., and Simmer, C.: A network suitable microwave radiometer for operational monitoring of the cloudy atmosphere, Atmos. Res., 75, 183–200, doi:10.1016/j.atmosres.2004.12.005, 2005. 2859

Rosenkranz, P. W.: Absorption of microwaves by atmospheric gases, in: Atmospheric Remote Sensing by Microwave Radiometry, edited by: Janssen, M. A., John Wiley & Sons, 37–90, New York, 1993. 2867, 2884

Rosenkranz, P. W.: Water vapor microwave continuum absorption: a comparison of measurements and models, Radio Sci., 33, 919–928, 1998. 2867, 2889

Scheiben, D., Straub, C., Hocke, K., Forkman, P., and Kämpfer, N.: Observations of middle atmospheric H_2O and O_3 during the 2010 major sudden stratospheric warming by a network of microwave radiometers, Atmos. Chem. Phys., 12, 7753–7765, doi:10.5194/acp-12-7753-2012, 2012. 2876

Scherhag, R.: Die explosionsartigen Stratosphärenerwärmungen des Spätwinters, 1951–52, Ber. Deut. Wetterdienst, 38, 51–63, 1952. 2876

Shvetsov, A. A., Fedoseev, L. I., Karashtin, D. A., Bol'shakov, O. S., Mukhin, D. N., Skalyga, N. K., and Feigin, A. M.: Measurement of the middle-atmosphere temperature profile using a ground-based spectroradiometer facility, Radiophys. Quantum El., 53, 321–325, 2010. 2859

AMTD
6, 2857–2905, 2013

Straub, C., Murk, A., and Kämpfer, N.: MIAWARA-C, a new ground based water vapor radiometer for measurement campaigns, Atmos. Meas. Tech., 3, 1271–1285, doi:10.5194/amt-3-1271-2010, 2010. 2859

Ware, R., Carpenter, R., Güldner, J., Liljegren, J., Nehrkorn, T., Solheim, F., and Vandenberghe, F.: A multichannel radiometric profiler of temperature, humidity, and cloud liquid, Radio Sci., 38, 44.1–44.13, doi:10.1029/2002RS002856, 2003. 2859

Waters, J. W.: Ground-based measurement of millimetre-wavelength emission by upper stratospheric O_2, IEEE T. Geosci. Remote, 44, 1075–1092, doi:10.1109/TGRS.2006.873771, 1973. 2859

Waters, J. W., Froidevaux, L., Harwood, R. S., Jarnot, R. F., Pickett, H. M., Read, W. G., Siegel, P. H., Cofield, R. E., Filipiak, M. J., Flower, D. A., Holden, J. R., Lau, G. K. K., Livesey, N. J., Manney, G. L., Pumphrey, H. C., Santee, M. L., Wu, D. L., Cuddy, D. T., Lay, R. R., Loo, M. S., Perun, V. S., Schwartz, M. J., Stek, P. C., Thurstans, R. P., Boyles, M. A., Chandra, K. M., Chavez, M. C., Chen, G. S., Chudasama, B. V., Dodge, R., Fuller, R. A., Girard, M. A., Jiang, J. H., Jiang, Y. B., Knosp, B. W., LaBelle, R. C., Lam, J. C., Lee, K. A., Miller, D., Oswald, J. E., Patel, N. C., Pukala, D. M., Quintero, O., Scaff, D. M., Van Snyder, W., Tope, M. C., Wagner, P. A., and Walch, M. J.: The Earth Observing System Microwave Limb Sounder (EOS MLS) on the Aura satellite, IEEE T. Geosci. Remote, 44, 1075–1092, doi:10.1109/TGRS.2006.873771, 2006. 2859

AMTD
6, 2857–2905, 2013

Table 1. Specifications of TEMPERA.

Optical system	Corrugated horn antenna with parabolic mirror, HPBW = 4°
Receiver type	Uncooled heterodyne receiver, filterbank; digital FFT spectrometer
RF frequency range	Filterbank: 51–57 GHz, FFT spectrometer: 52.4–53.2 GHz
Receiver operation mode	Single-Side Band
Receiver noise temperature	475–665 K
Filterbank	4 filters, bandwidth 250 MHz and 1 GHz
FFT Spectrometer	Bandwidth 1 GHz, resolution 30.5 kHz, 32 768 channels
Mixer (FFT-Backend)	I/Q
Calibration	Hot load, noise diode

AMTD
6, 2857–2905, 2013

Table 2. Specifications of the 12 tropospheric channels (ch1–ch12) and of the FFT spectrometer (ch_fft) with frequency f, the bandwidth B and receiver noise temperature T_N.

channel	f [GHz]	B [MHz]	T_N [K]
1	51.25	250	475
2	51.75	250	540
3	52.25	250	585
4	52.85	250	495
5	53.35	250	550
6	53.85	250	555
7	54.40	250	480
8	54.90	250	560
9	55.40	250	570
10	56.00	1000	555
11	56.50	1000	625
12	57.00	1000	665
fft	52.4–53.2	800	480

AMTD
6, 2857–2905, 2013

Table 3. List of used line parameters for O_2. The data are from the PWR93 oxygen absorption model (Rosenkranz, 1993).

Quantum ID	ν [GHz]	S (300 K) [cm^2 Hz]	b [ ]	w [MHz hPa^{-1}]	y [10^{-3} hPa^{-1}]	v [10^{-3} hPa^{-1}]
29-	52.5424	0.4264×10^{-16}	6.004	0.94	0.7702	0.6526
27-	53.0669	0.8898×10^{-16}	5.224	0.97	0.7348	0.6206

AMTD
6, 2857–2905, 2013

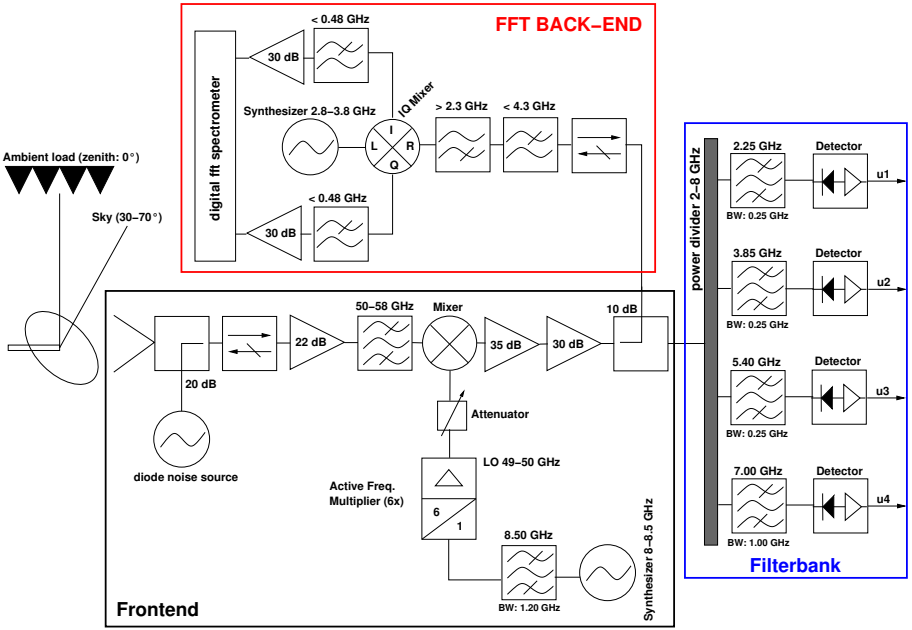

Fig. 1. TEMPERA block diagram.

AMTD
6, 2857–2905, 2013

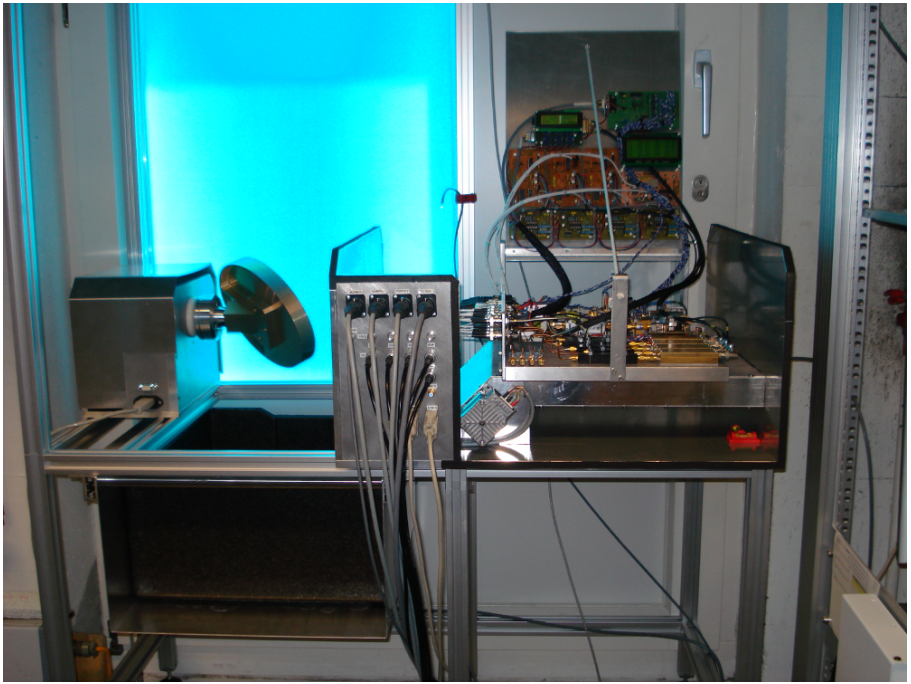

Fig. 2. TEMPERA with its main components, the frontend and the parabolic mirror. TEMPERA is 1.1 m wide. The instrument is placed inside in a thermally controlled lab in front of a blue styrofoam window through which the atmosphere is observed.

AMTD
6, 2857–2905, 2013

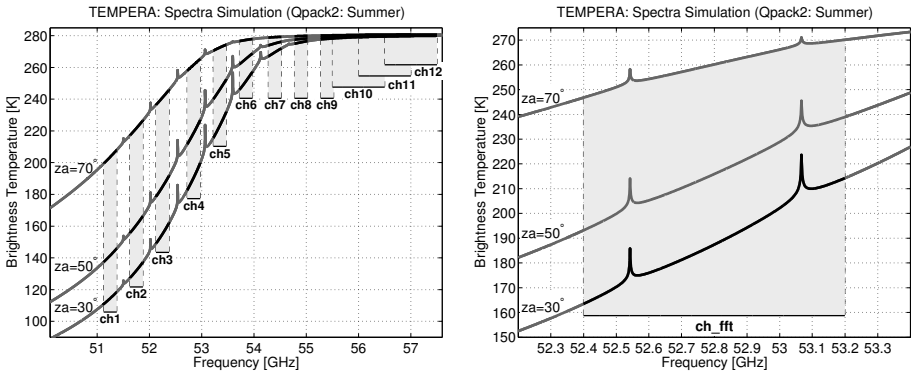

Fig. 3. Left panel: TEMPERA spectrum from 51–57 GHz simulated with Qpack2/ARTS2 during summer for zenith angles at 30°, 50° and 70°. The grey bars indicate the 12 channels (ch1–ch12) of the filterbank. Right panel: spectrum from 52–53 GHz simulated with Qpack2/ARTS2 during summer for zenith angles of 30°, 50° and 70°. The grey bar indicates the available bandwidth of the FFT spectrometer (ch_fft).

AMTD
6, 2857–2905, 2013

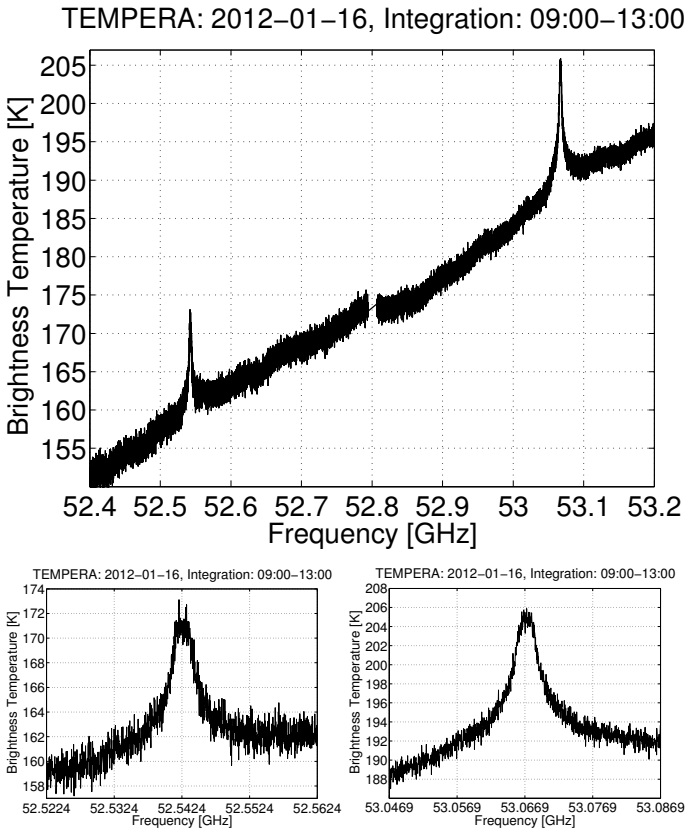

Fig. 4. Spectrum of brightness temperatures measured with TEMPERA on 16 January 2012 from 9:00–13:00 (UT). Upper panel: the whole FFT spectrum, with all channels from 52.4 to 53.2 GHz. The gap in the middle is due to effects of the filters. Lower panels: zoomed spectra around the first line at 52.5424 GHz and the second line at 53.0669 GHz.

AMTD
6, 2857–2905, 2013

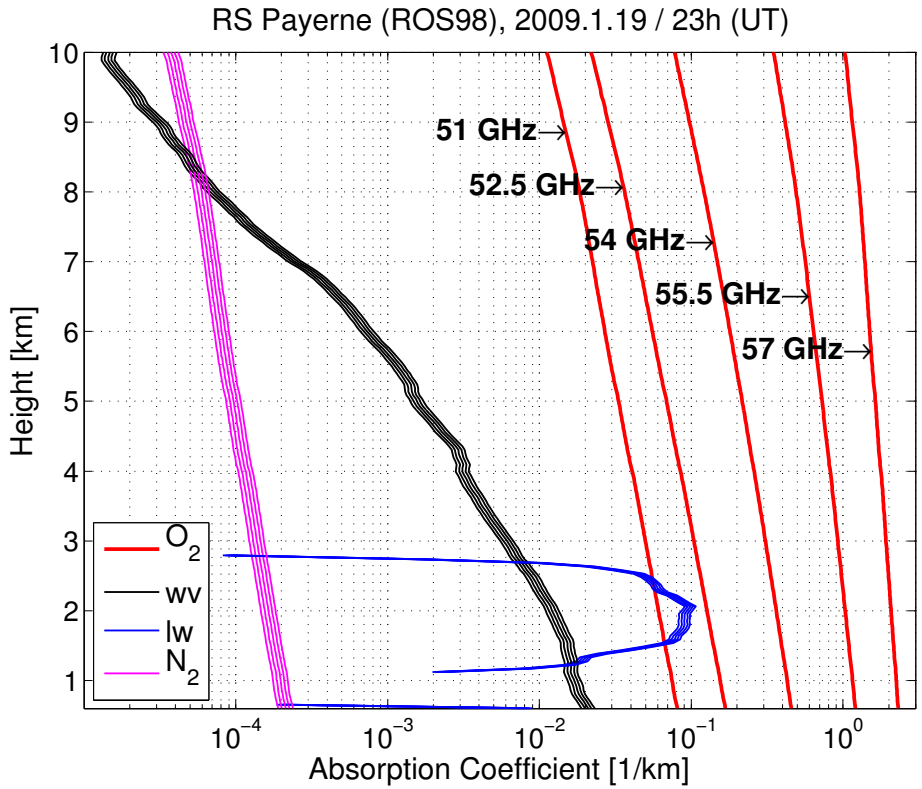

Fig. 5. Absorption Coefficient versus height for oxygen (O_2), water vapor (wv), liquid water (lw) and nitrogen (N_2) at 51, 52.5, 54, 55.5 and 57 GHz calculated with radiosonde data from Payerne on 19 January 2009 (IWV = 13.11 mm, ILW = 0.19 mm). Calculations with the Rosenkranz (1998) Model.

AMTD
6, 2857–2905, 2013

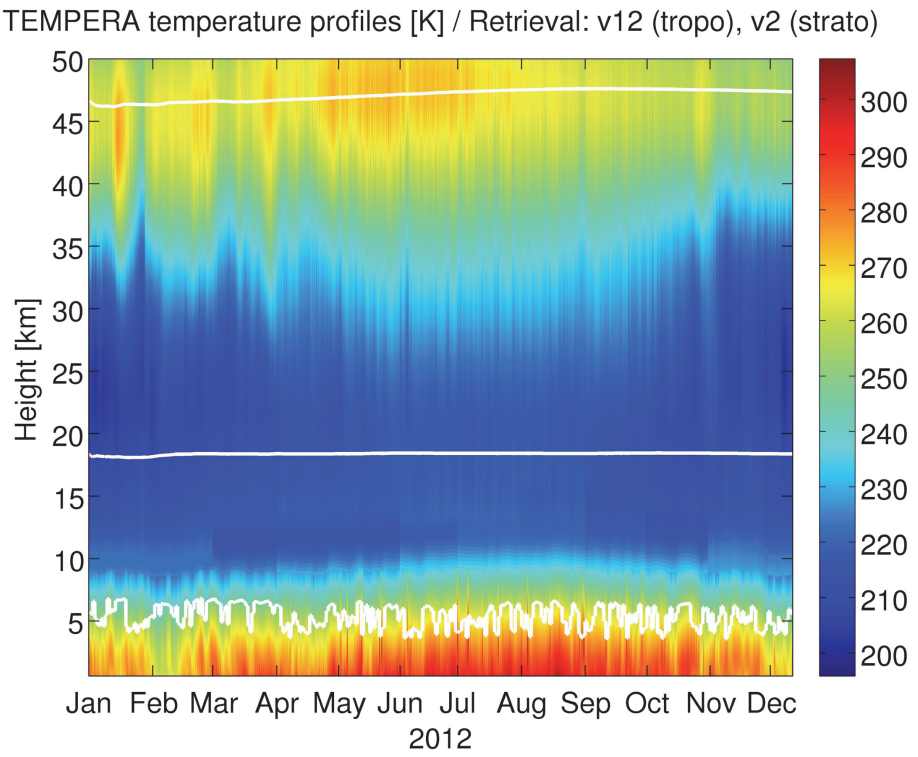

Fig. 6. Temperature profiles derived from TEMPERA from ground to 50 km from 1 January to 13 December 2012. The white lines indicate the region where MR = 0.6.

AMTD
6, 2857–2905, 2013

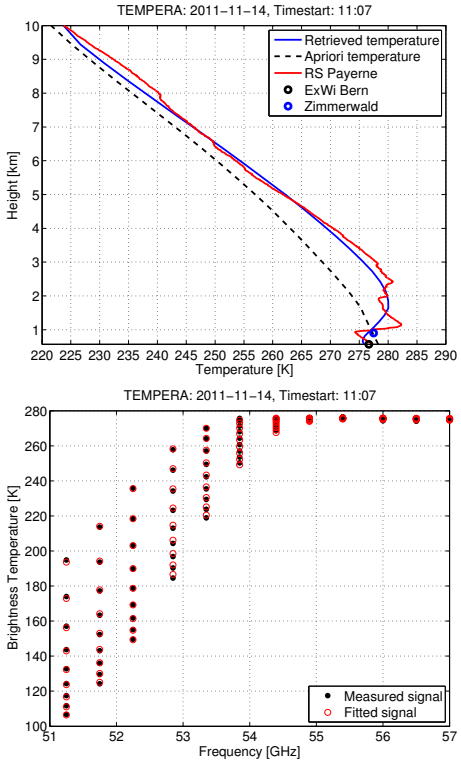

Fig. 7. Measurement of 14 November 2011 at 11:07–11:22 (UT) during clear sky (ILW = 0 mm). Upper panel: retrieved temperature profile (blue line). The a-priori profile is the dashed black line. Comparison with radiosonde data from Payerne (red line) and with weather station data from Bern (black circle), Zimmerwald (blue circle). Lower panel: brightness temperatures of 12 channels measured with TEMPERA (black) compared with the forward model brightness temperatures (red) corresponding to the retrieval.

AMTD
6, 2857–2905, 2013

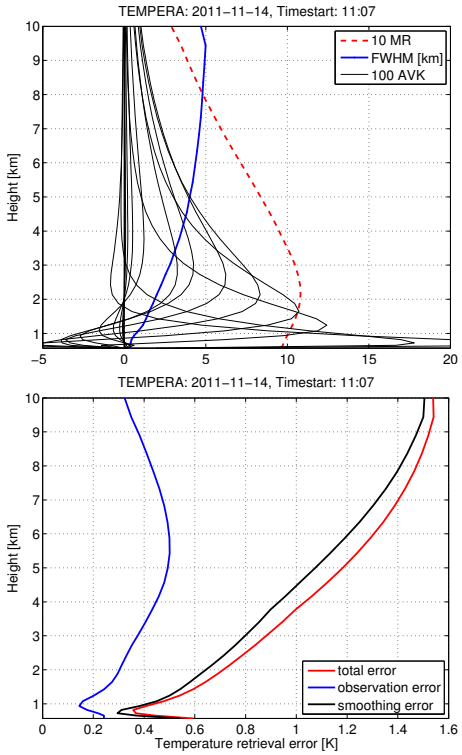

Fig. 8. Measurements of 14 November 2011 at 11:07–11:22 (UT) during clear sky (ILW = 0 mm). Upper panel: the averaging kernels (AVK, plotted every 4th) of TEMPERA are shown in this plot together with the measurement response (MR) and the full-width at half-maximum (FWHM, in km). Lower panel: error of the retrieval. The error statistics contain the total error (red) consisting of observation error (blue) and smoothing error (black).

AMTD
6, 2857–2905, 2013

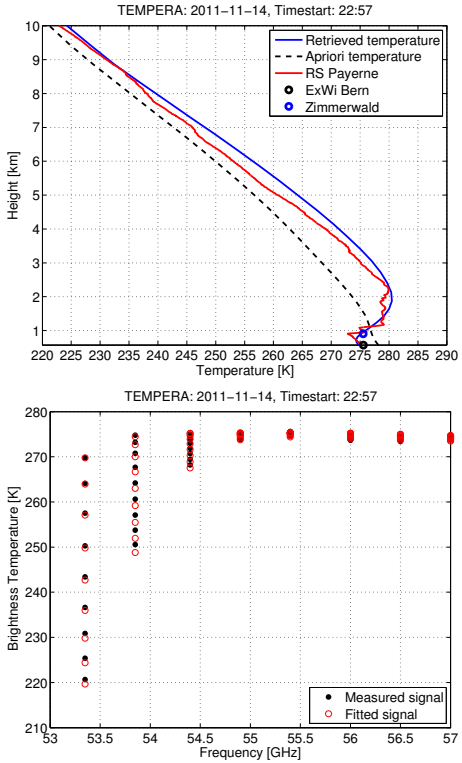

Fig. 9. Measurement of 14 November 2011 at 22:57–23:12 (UT) during cloudy sky (ILW = 0.1 mm). Upper panel: temperature profile (blue line) retrieved with TEMPERA. The a-priori profile is the dashed black line. The retrieved profile is compared with radiosonde data from Payerne (red line) and with weather station data from Bern (black circle), Zimmerwald (blue circle). Lower panel: brightness temperatures of 8 channels measured with TEMPERA (black) compared with the forward model brightness temperatures (red) corresponding to the retrieval.

AMTD
6, 2857–2905, 2013

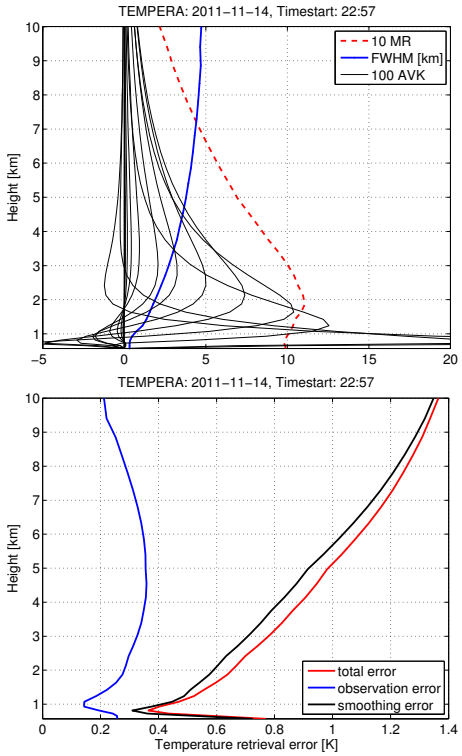

Fig. 10. Measurement of 14 November 2011 at 22:57–23:12 (UT) during cloudy sky (ILW = 0.1 mm). Upper panel: the averaging kernels (AVK, plotted every 4th) of TEMPERA are shown in this plot together with the measurements response (MR) and the full-width at half-maximum (FWHM, in km). Lower panel: error of the retrieval. The error statistics contain the total error (red), consisting of observation error (blue) and smoothing error (black).

AMTD
6, 2857–2905, 2013

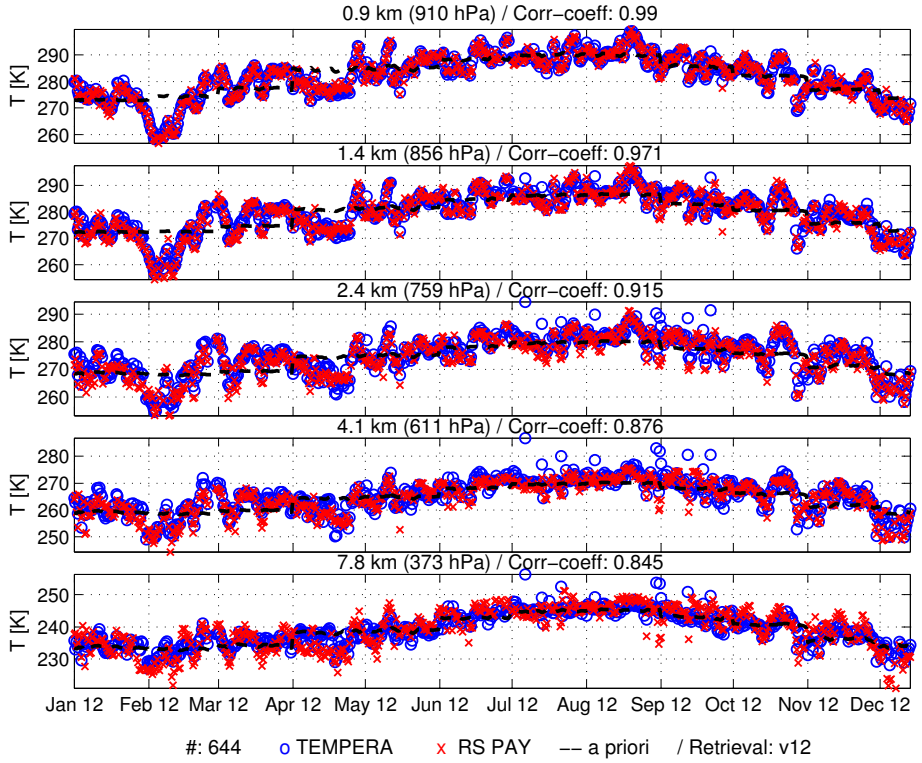

Fig. 11. Time-series from 1 January to 13 December 2012 (644 profiles) of tropospheric temperature profiles from TEMPERA (blue) compared with radiosonde data from Payerne (red, regridded to TEMPERA grid) for five different altitude levels. The black dashed line is the a-priori.

AMTD
6, 2857–2905, 2013

Microwave radiometer to retrieve temperature profiles

O. Stähli et al.

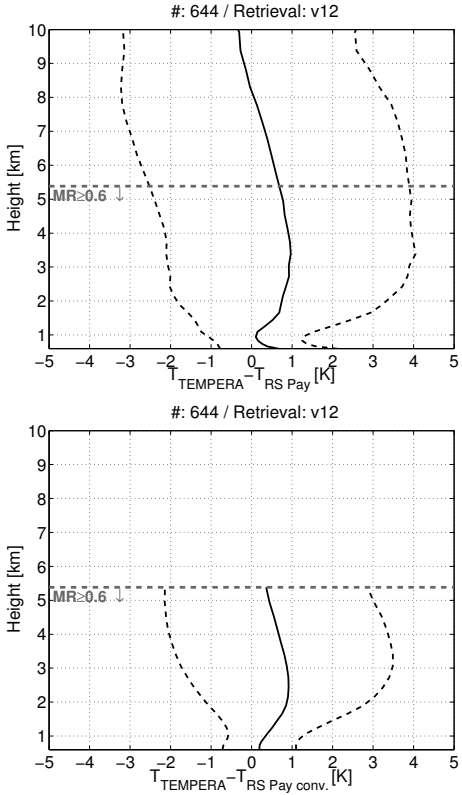

Fig. 12. Comparison of 644 profiles (1 January to 13 December 2012) between TEMPERA and radiosonde data from Payerne over an altitude range from ground (0.575 km) to 10 km. Plotted is the mean (black line) and the standard deviation (black dashed line) of the difference between TEMPERA and radiosonde data from Payerne. The horizontal grey line indicates the region where MR = 0.6. Upper panel: TEMPERA compared with unconvolved radiosonde data from Payerne. Lower panel: TEMPERA compared with convolved radiosonde data from Payerne over a altitude region with MR ≥ 0.6.

AMTD
6, 2857–2905, 2013

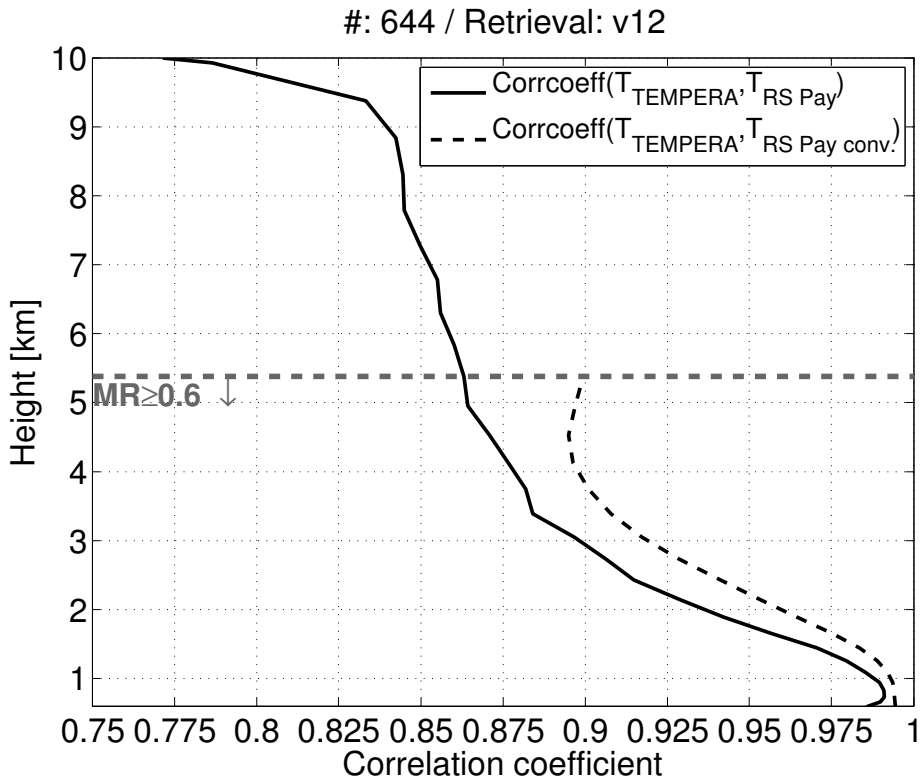

Fig. 13. Correlation coefficient of the comparison for 644 profiles (1 January to 13 December 2012) between TEMPERA and radiosonde data from Payerne over an altitude range from ground (0.575 km) to 10 km. The horizontal grey line indicates the region where MR = 0.6. Correlation coefficient of the comparison between TEMPERA and the unconvolved (black line) and convolved (dashed black line, altitude region with MR ≥ 0.6) radiosonde data from Payerne.

AMTD
6, 2857–2905, 2013

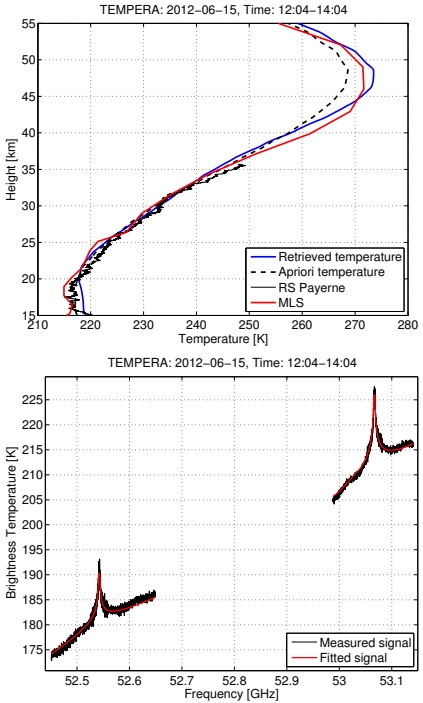

Fig. 14. Measurement of 15 June 2012 from 12:04–14:04 (UT) during clear sky (ILW = 0 mm). Upper panel: temperature profile (blue line) retrieved with TEMPERA spectrometer measurements. The a-priori profile is the dashed black line. The retrieved profile is compared with radiosonde data from Payerne (black line) and with MLS data (red). Lower panel: brightness temperatures measured with TEMPERA (black) compared with the forward model brightness temperatures (red) that we received with the retrieval. In the forward model ±1 MHz around the two line centers we have no frequencies points in the grid, because until now the Zeeman effect has not been incorporated in Qpack2/ARTS2. In the center of the lines (±16 MHz, 1000 channels) we use all channels and on the wings of the line we use a binning of 3 channels for data reduction.

AMTD
6, 2857–2905, 2013

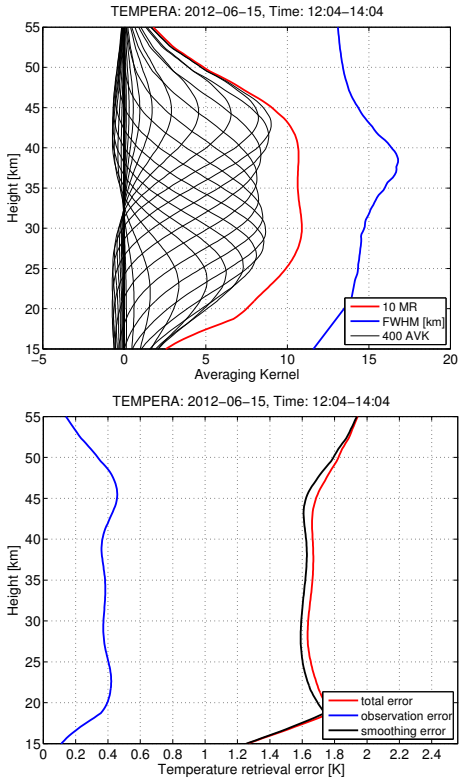

Fig. 15. Measurement of 15 June 2012 from 12:04–14:04 (UT) during clear sky (ILW = 0 mm). Upper panel: the averaging kernels (AVK, plotted every 7th) of TEMPERA are shown in this plot together with the measurements response (MR) and the full-width at half-maximum (FWHM, in km). Lower panel: error of the retrieval. The error statistics contain the total error (red), consisting of observation error (blue) and smoothing error (black).

AMTD
6, 2857–2905, 2013

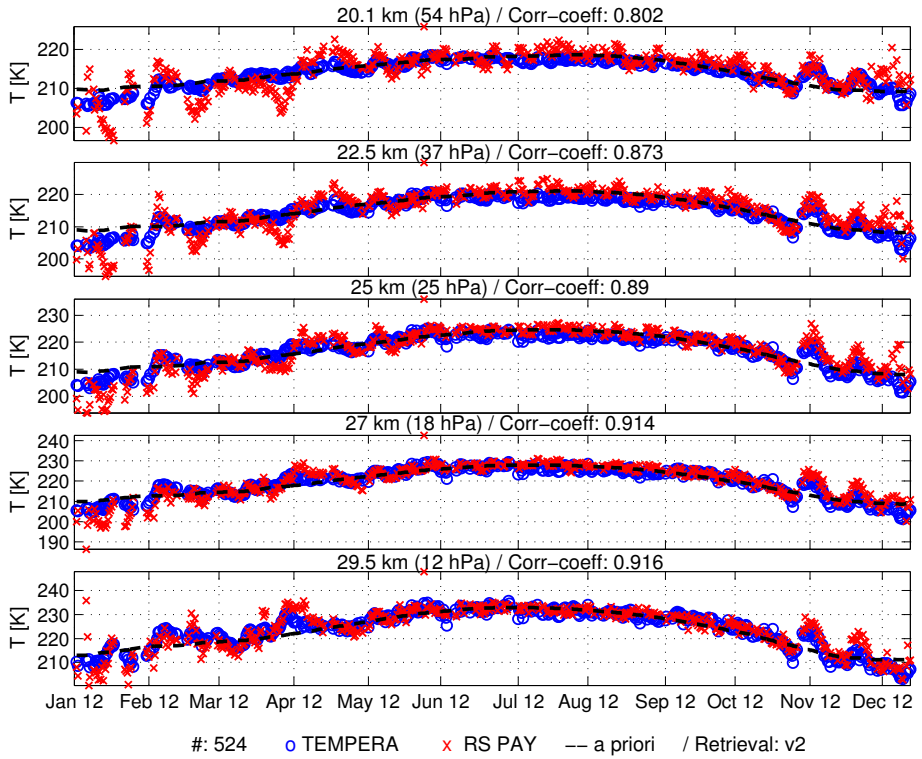

Fig. 16. Timeseries (524 profiles) of stratospheric temperature profiles from TEMPERA (blue) compared with radiosonde data from Payerne (red, regridded to TEMPERA grid) for five different altitude levels. The black dashed line is the a-priori.

AMTD
6, 2857–2905, 2013

Microwave radiometer to retrieve temperature profiles

O. Stähli et al.

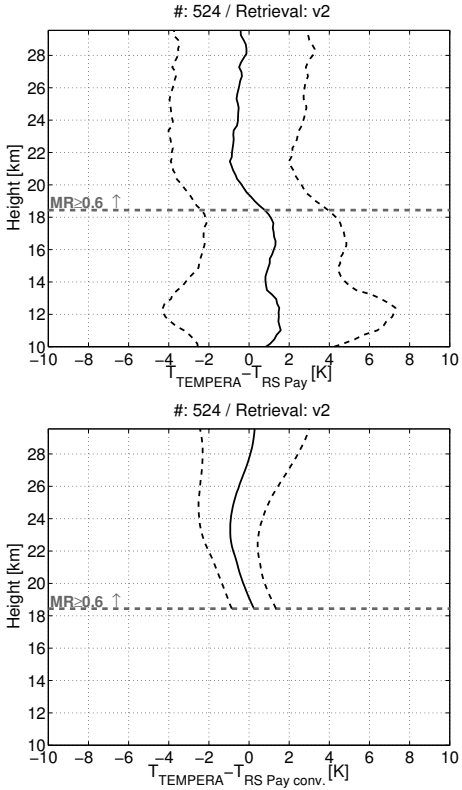

Fig. 17. Comparison of 524 profiles (1 January to 13 December 2012) between TEMPERA and radiosonde data from Payerne over an altitude range from 10 km to about 29 km. Plotted is the mean (black line) and the standard deviation (black dashed line) of the difference between TEMPERA and radiosonde data from Payerne. The horizontal grey line indicates the region where MR = 0.6. Upper panel: TEMPERA compared with unconvolved radiosonde data from Payerne. Lower panel: TEMPERA compared with convolved radiosonde data from Payerne over a altitude region with MR ≥ 0.6.

AMTD
6, 2857–2905, 2013

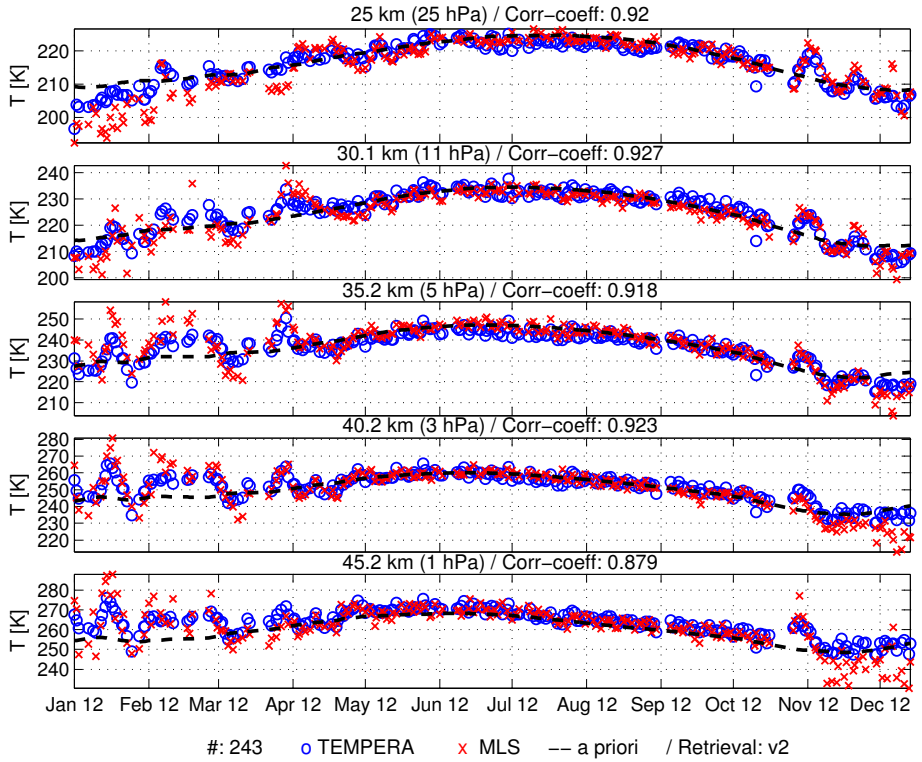

Fig. 18. Timeseries (243 profiles) of stratospheric temperature profiles from TEMPERA (blue) compared with MLS data (red, regridded to TEMPERA grid) for five different altitude levels. The black dashed line is the a-priori.

AMTD
6, 2857–2905, 2013

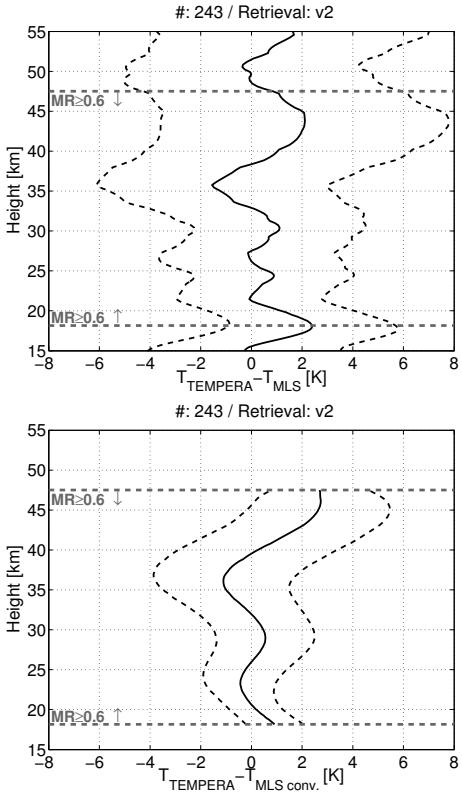

Fig. 19. Comparison of 243 profiles (1 January to 13 December 2012) between TEMPERA and MLS data over an altitude range from 15 km to about 55 km. Plotted is the mean (black line) and the standard deviation (black dashed line) of the difference between TEMPERA and MLS data. The horizontal grey lines indicate the region where MR = 0.6. Upper panel: TEMPERA compared with unconvolved MLS data. Lower panel: TEMPERA compared with convolved MLS data over a altitude region with MR ≥ 0.6.

AMTD
6, 2857–2905, 2013

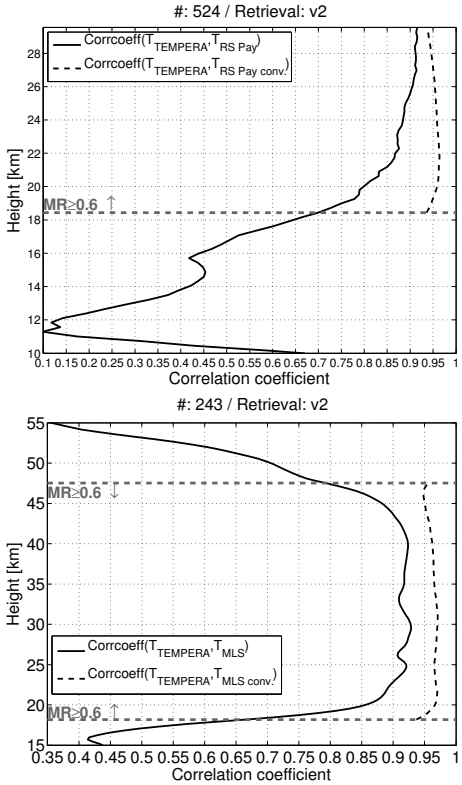

Fig. 20. Correlation coefficient of the comparison between TEMPERA and radiosonde data from Payerne (upper panel, 524 profiles) and MLS data (lower panel, 243 profiles) during the period from 1 January to 13 December 2012. The horizontal grey lines indicate the region where MR = 0.6. Correlation coefficient of the comparison between TEMPERA and the unconvolved (black line) and convolved data (dashed black line, altitude region with MR ≥ 0.6).

AMTD
6, 2857–2905, 2013

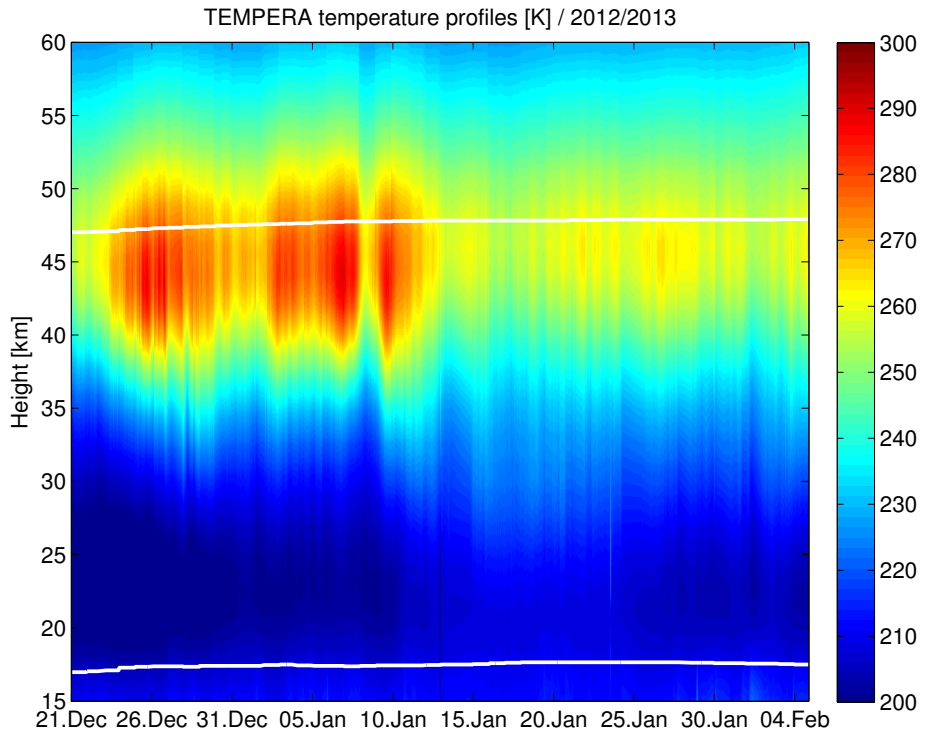

Fig. 21. Retrieved temperature profiles from 15 to 60 km from 21 December 2012 to 4 February 2013 (46 days). The white lines indicate the region where MR = 0.6.

AMTD
6, 2857–2905, 2013

Microwave radiometer to retrieve temperature profiles

O. Stähli et al.